PHYSICAL REVIEW A VOLUME 34, NUMBER 4 OCTOBER 1986

Bound excited states of HeH: Predissociation of $A\,^2\Sigma^+$ and radiative dissociation from $B\,^2\Pi$

J. R. Peterson and Y. K. Bae
Chemical Physics Laboratory, SRI International, Menlo Park, California 94025
(Received 30 June 1986)

Bound excited states of HeH, formed by electron capture in a beam of 6-keV HeH^+ ions passing through Cs vapor, were observed to undergo both predissociation and radiative dissociation. Measurement of the kinetic energy spectrum of the H-atom products was facilitated by their conversion to H^-. Transformation of the laboratory energy spectrum to the 0° and 180° center-of-mass energy release spectra reveals a broad peak at about 8.4 eV, consistent with predissociation from several vibrational levels of the $A\,^2\Sigma^+$ state, and a lower peak at about 3.3 eV, resulting from the $B\,^2\Pi \rightarrow X\,^2\Sigma^+$ radiative decay recently observed by Möller, Beland, and Zimmerer.

Although bound states of electronically excited HeH were first predicted theoretically in 1963 by Michels and Harris,[1] and other calculations followed,[2,3] only very recently have any experimental observations been made. The potential energy curves of several electronic states, shown in Fig. 1, were drawn to fit the several points calculated by Theodorakopoulos *et al.*[3] Möller, Beland, and Zimmerer[4] first observed radiation from the $B\,^2\Pi \rightarrow X\,^2\Sigma^+$ transition following reactions between He and electronically excited H_2. They assumed that the $A\,^2\Sigma^+$ state was also populated but predissociates. Shortly thereafter, Ketterle, Figger, and Walther[5] observed emissions from excited HeH produced in electron capture by 15-keV HeH^+ ions in alkali vapor, and were able to deduce some related molecular constants, assigning these emissions to $C\,^2\Sigma^+ \rightarrow A\,^2\Sigma^+$ transitions.

To observe simultaneously the effects of predissociations and radiative dissociations from these states, we produced them in a 6-keV beam by near-resonant electron capture of HeH^+ in Cs and used a recently developed technique to observe the dissociation fragments.[6] The results reveal radiative dissociation from $B\,^2\Pi$ and predissociation of $A\,^2\Sigma^+$, confirming the assumptions of Möller *et al.*,[4] and are consistent with the most recently calculated potentials.[3]

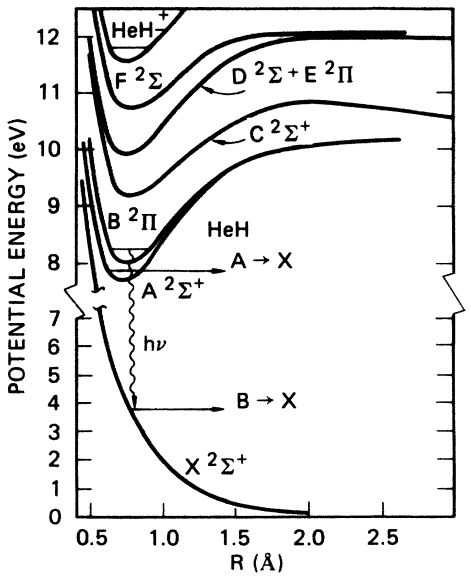

FIG. 1. Potential energies of HeH and HeH^+ (from Ref. 3). Examples of kinetic energies released in $A \rightarrow X$, predissociation, and $B \rightarrow X$, radiative dissociation, are given by the horizontal arrows.

We have previously used the experimental method to determine the final states produced in electron capture by H_2^+, H_3^+, and O_2^+ in Cs.[6] In the work described here, we examined the products of the reaction

$$HeH^+ + Cs \rightarrow HeH^* , \tag{1a}$$

followed by either predissociation

$$HeH^* \rightarrow H + He , \tag{1b}$$

or radiative dissociation

$$HeH^* \rightarrow HeH(X) + h\nu \rightarrow H + He . \tag{1c}$$

Near-resonant electron capture reactions in step (1a) favor the population of excited states HeH* that lie about 3.9 eV (the ionization potential of Cs) below the energy of the parent HeH^+ ion, if they also have favorable Franck-Condon factors with HeH^+. These conditions are best satisfied by the $A\,^2\Sigma^+$ and $B\,^2\Pi$ states, which should dominate the products of (1a); however, higher states are expected in smaller amounts.

In the experiment, we seek to determine the spectrum of W, the total center-of-mass (c.m.) kinetic energy given to the dissociation products H and He in each reaction. For the predissociation reactions (1b), $W = E(HeH^*)$, the entire excitation energy of HeH*. For radiative dissociation (1c), the values of W are reduced by the photon energies $h\nu$. Examples for the predissociation of $A\,^2\Sigma^+$ ($v'=0$) and radiative dissociation of $B\,^2\Pi$ ($v'=0$) are given by the horizontal arrows in Fig. 1. In this method[6] we actually measure the kinetic energies of H^- ions produced at 0° laboratory angle by the H-atom products of reactions (1b) and (1c), in subsequent electron-capture collisions with Cs atoms in the oven. These ions thus represent H atoms ejected in the dissociation at 0° and 180° c.m.

The laboratory energy spectrum of the H^- ions is shown in Fig. 2. In the dissociation of a diatomic molecule of

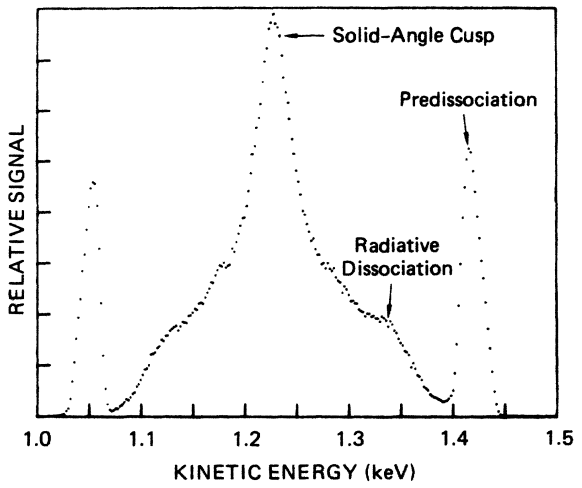

FIG. 2. Laboratory energy spectrum of H^- from H-atoms dissociation products in a 6.142-keV beam of HeH*, observed at 0°.

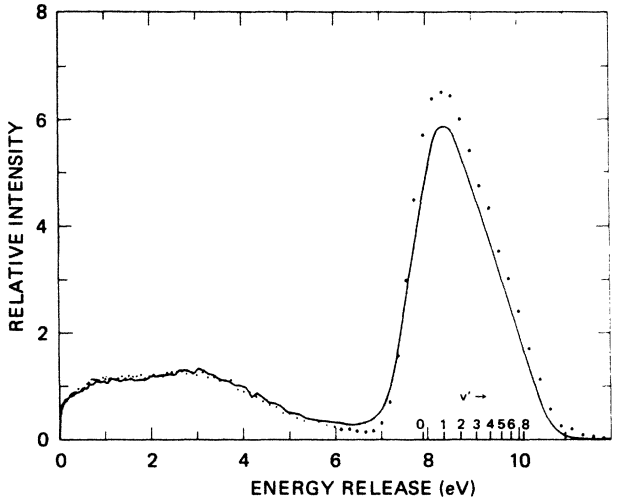

FIG. 3. The spectrum in Fig. 2 transformed into total c.m. energies released in dissociation. Solid line and dots are 0° and 180° c.m. data, respectively. Locations of the $J=0$ energies from $A\,^2\Sigma^+$ ($v'=0\rightarrow 8$) predissociation are indicated.

mass m_1+m_2 and energy E_0, the fragments of mass m_1, whose trajectories are at 0° laboratory angle, have energies given by

$$E_1=(m_1+m_2)^{-1}[m_1E_0+m_2W\pm 2(m_1m_2E_0W)^{1/2}]. \quad (2)$$

The spectrum is centered about a peak at energy $m_1E_0/(m_1+m_2)$, which occurs because of a cusp in the c.m. solid angle subtended by the detector when $W=0$. The c.m. energy release distributions are determined from

$$d^2\sigma/dW\,d\Omega_c=(\mu/m_1)^{3/2}(W/E_1)^{1/2}d^2\sigma/dE_1\,d\Omega_1, \quad (3)$$

where $\mu=m_1m_2/(m_1+m_2)$.[7]

In addition to this solid angle effect, the detection efficiency is also proportional to the laboratory energy E_1 because the relative energy resolution $\Delta E/E$ of the analyzer (as operated here) is constant. Furthermore, the probability of the H atoms being converted H^- is proportional to σ_{0-1}, the total cross section for the process $H+Cs\rightarrow H^-+Cs^+$, which has been measured by Miethé, Dreiseidler, and Salzborn.[8] To account for these two effects, the intensities in Fig. 2 were divided by the product $E_1\sigma_{0-1}$ before being transformed into the c.m. system according to Eq. (3). The two components of the transformed spectra representing the 0° and 180° contributions are shown in Fig. 3. The 0° and 180° c.m. spectra in Fig. 3 both show a large, high-energy peak centered at about 8.4 eV, resulting from predissociation, and a lower, broader peak centered at about 3 eV, from radiative transitions to the repulsive ground state. The radiative dissociation spectrum is naturally a continuum, but the predissociation peak is evidently broadened by contributions from several energy levels.

In analyzing our data, we assumed not only that near-resonance conditions would ensure that only the A and B electronic states of HeH contributed substantially to our data, but that vibrational excitation would exist in the HeH products. Following the assumptions of Möller *et al.*,[4] which were supported by a preliminary analysis of our data, we also assumed that the A state predissociates, and the B state radiates. We shall discuss these assumptions later. Our analysis made use of energy levels and vibrational wave functions that were obtained[9] from A- and B-state potentials determined by spline fits to the values at several internuclear distances calculated by Theodorakopoulos *et al.*[3] The goal was to convolve the individual spectra from the contributions of several vibrational levels of the A and B states into simulated spectra that matched the data.

To consider contributions to the predissociation peak from different vibrational levels of the $A^2\Sigma^+$ state, the high-energy data in Fig. 2 between 1.35 and 1.45 keV were plotted, and the tail of the radiative continuum was extrapolated so that it gradually reached zero at about 1.42 keV. This curve was subtracted from the predissociation peak, yielding the remainder shown as the crossed curve in Fig. 4. Also indicated in Fig. 4 are the energies corresponding to H atoms that would result from 0° predissociations of the individual vibrational levels $v'=0\rightarrow 8$ of the $A^2\Sigma^+$ state. The ratio $\Delta E/E$ intrinsic to the energy analyzer should be about 0.004 FWHM (full width at half maximum) for the 0.5-mm-diam apertures that were used. However, collisional effects, particularly the angular scattering mentioned above, are expected to increase the width, which was therefore unknown. In fitting the summed contributions $I(v')$ from different vibrational levels v', it was reasonable to approximate the analyzer function by a Gaussian of undetermined width, to account for scattering effects. However, the spacings of the kinetic energies from the successive v' are smaller than even the 0.4% theoretical width of the analyzer. This condition precludes the observation of substructure, and prevents a unique determination of the individual contributions $I(v')$ by a least-squares fit. To reduce the number of variables, we included the $I(v')$ from $v'=0\rightarrow 7$ in four successive pairs of convolved Gaussians separated by the appropriate energy spacings in the A state. The widths were linked,

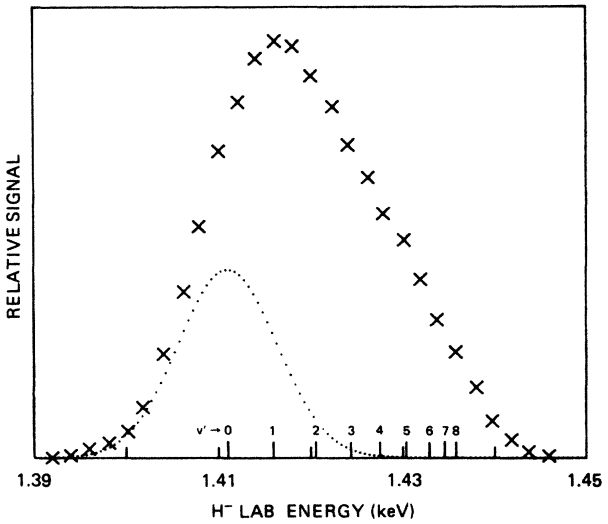

FIG. 4. High laboratory-energy predissociation peak in Fig. 2 with the tail of the low-energy continuum subtracted. Locations of the centers of the energy distributions from various $A^2\Sigma^+$ vibrational levels are indicated. The distribution from $v'=0$ determined by the fitting procedure is shown by the dots.

but were allowed to vary. The amplitudes in each pair were in fixed but adjustable ratios. Least-squares fits to the data then converged satisfactorily.

For the case of equal amplitudes *within each pair,* and equal widths for all Gaussians, the fit yielded the relative amplitudes 1, 0.62, 0.12, and 0.15 for the pairs $v'=0+1$, $2+3$, $4+5$, and $6+7$, respectively. The relative width $\Delta E/E$ of each Gaussian was found to be 0.9% FWHM, which is over twice the instrumental value 0.4%, showing that scattering effects controlled the effective width. The contribution from $v'=0$ is shown as the dotted curve in Fig. 4. Several fits were made to explore the effects of changing the ratios of amplitudes within each pair. The variances (χ^2's) of the fits changed some as these ratios were varied, as did the relative amplitudes, but the widths were always about the same. The results indicated above are reasonable and representative of the other results, and give a qualitative indication of the vibrational excitation that existed in the A state.

To simulate the low energy-release continuum from $B^2\Pi \rightarrow X$ radiative transitions, we approximated the relative transition probabilities from each level $v'=0 \rightarrow 7$, as functions of the internuclear separation R, by

$$P(v',R)=\nu(R)^3\psi^2(v',R)[d\nu(R)/dR]^{-1} , \quad (4)$$

where $\nu(R)$ is the frequency of the radiation, given by

$$h\nu(R)=V_B(R)-V_X(R) \quad (5)$$

(h is Planck's constant) and $\psi(v',R)$ is the appropriate B-state vibrational wave function. Note that the initial vibrational energy is conserved, and does not appear in Eq. (5). Equation (4) is based on the classical Franck-Condon principle,[10,11] and assumes that the electronic dipole matrix element is independent of R. By conservation of energy, the kinetic energy released by a transition at R is

$$W(R)=E_B(v')-h\nu(R) , \quad (6)$$

where $h\nu(R)$ is given by Eq. (5), and $E_B(v')$ is the total energy of the molecule in the v' level of $B^2\Pi$ (relative to the separated atom limit). The "reflection" converts $P(v',R)$ into $P(v',h\nu)$ (the distribution of photon energies) by determining $R(h\nu)$ from (5). Similarly, we find $P(v',W)$ the distribution of W produced from each v', by determining $R(W)$ from (6).

The predicted energy release spectrum from $v'=0$ of the B state is fairly Gaussian shaped, centered at 3.3 eV with $\Delta W=2.2$ eV FWHM. Radiation from higher levels is structured according to the maxima in $\psi^2(v',R)$ and strongly weighted at the outer turning point (low-energy release). Contributions from excited levels therefore constitute the lower end of the spectrum in Fig. 3. Different combinations of calculated spectra from levels $v'=0-7$ were summed and compared to the data. The combined simulated spectra could easily approximate the low-energy observed spectrum, but were too low in the high-energy tail of the continuum.

Because of the uncertainties in the vibrational wave functions and the effective analyzer transmission function, further analysis is not warranted. We have not included the effects of rotational energies because they seemed unlikely to be important enough to compete with vibrational effects. Ketterle *et al.*,[5] who formed their excited neutral beams in a similar manner, fitted their HeD spectra with a rotational temperature of 3100 K, or about 0.3 eV. However the deconvoluted A-state peak in Fig. 3 has $\Delta W \simeq 2$ eV FWHM, thus vibrational excitation must be primarily responsible. Furthermore, since rotational energies can only add to W, the low-energy end of the B-state radiative dissociation continuum must also result from excited vibrational levels.

We now consider the $A^2\Sigma^+$ and $B^2\Pi$ contributions to the data. First, their production is favored over others because electron capture by molecular ions (at these velocities) has a strong propensity for final states that are nearly resonant and have reasonably good Franck-Condon factors with the parent ions.[6,12] The A state is closely resonant with Cs in reaction (1a), and its molecular constants are very similar to those of HeH^+. Reactions to the B state are 0.4 eV endoergic for $v=0$, and its Franck-Condon factors with HeH^+ are probably smaller, but it clearly contributes. The C state, however, observed by Ketterle *et al.*,[5] is energetically about 1.5 eV higher than the A state and it should constitute only a minor fraction of the beam; in any case, it radiates rapidly to the A state. Predissociation of the A state is fully allowed and should be much more rapid than radiation. Broadening of $^2\Pi \rightarrow A^2\Sigma$ radiative transition spectra in ArH was observed by Johns,[13] who deduced A-state predissociation lifetimes of $< 10^{-10}$ s. Thus the low-energy continuum should arise only from the fully allowed $B \rightarrow X$ radiative transition. Since predissociation of B can occur only through rotational (Coriolis) coupling and its potential surface is quite distant from that of the X state, B is quite likely to decay predominantly by radiation. We thus conclude that the A state essentially only

predissociates and the B state only radiates. The results support this conclusion as well as the calculated potential energies of the states,[3] and they confirm the assumptions of Möller *et al.*[4]

If the dissociations resulting from reactions (1b) and (1c) are isotropic in the c.m., as is probable, the areas under the two parts of the spectra in Fig. 3 representing predissociation and radiative dissociation should be good approximations to the relative populations of the $A\,^2\Sigma^+$ and $B\,^2\Pi$ states in the beam following the electron-capture reaction (1a). The areas are approximately in the ratio 2.3:1, which apparently results from the closer resonance conditions for the A state in this reaction as well as its better Franck-Condon factors with HeH^+.

During the final stages of preparing this paper, we were informed of results on the energy release spectra from HeH^+ charge transfer in Cs obtained by van der Zande *et al.*,[14] using the high-resolution neutral fragment spectrometer[12] at the FOM Laboratories in Amsterdam. Results from $^3HeD^+$ A-state predissociation showed distinct peaks, predominantly $v' \leq 3$, which were broadened by rotational excitation, apparently consistent with the 3100-K temperature found by Ketterle *et al.*[5] The results of our analysis would probably be improved by including this effect, but high values of v' would still be required to fit the low energies in the B-state continuum.

We thank Dr. Hanspeter Helm for calculating the vibrational energies and wave functions and Dr. David L. Huestis for several very helpful discussions. We are grateful to the National Science Foundation for its support under Grant No. PHY-8410980 and the Air Force Office of Scientific Research for its support under Contract No. F49620-85-0017.

[1]H. H. Michels and F. F. Harris, J. Chem. Phys. **39**, 1464 (1963).

[2]R. Polák, J. Vojtík, and I. Paidarovaí, Chem. Phys. **55**, 183 (1981); I. Paidarová, J. Vojtík, and R. Polák, *ibid.* **72**, 119 (1982).

[3]G. Theodorakopoulos, S. C. Farantos, R. J. Buenker, and S. D. Peyerimhoff, J. Phys. B **17**, 1453 (1984), and references therein.

[4]T. Möller, M. Beland, and G. Zimmerer, Phys. Rev. Lett. **55**, 2145 (1985).

[5]W. Ketterle, H. Figger, and H. Walther, Phys. Rev. Lett. **55**, 2941 (1985).

[6]J. R. Peterson and Y. K. Bae, Phys. Rev. A **30**, 2807 (1984).

[7]D. K. Gibson and J. Los, Physica **35**, 258 (1967); M. Vogler and W. Seibt, Z. Phys. **210**, 337 (1968); T. T. Wornock and R. B. Bernstein, J. Chem. Phys. **49**, 1878 (1968).

[8]K. Miethe, T. Dreiseidler, and E. Salzborn, J. Phys. B **15**, 3069 (1982).

[9]H. Helm (unpublished).

[10]E. U. Condon, Phys. Rev. **32**, 858 (1928).

[11]A. Gallagher, in *Excimer Lasers,* Topics in Applied Physics, Vol. 30 (Springer, New York, 1984), p. 139; J. Tellinghuisen, Adv. Chem. Phys. **60**, 299 (1985).

[12]D. P. deBruijn, J. N. Neuteboom, V. Sidis, and J. Los, Chem. Phys. **85**, 215 (1984).

[13]J. W. C. Johns, J. Mol. Spectrosc. **36**, 488 (1970).

[14]W. J. van der Zande, W. Koot, D. P. de Bruijn, and C. Kubach, Phys. Rev. Lett. **57**, 1219 (1986).